

Solvation of Sodium Octanoate Micelles in Concentrated Urea Solution Studied by Means of Molecular Dynamics Simulations

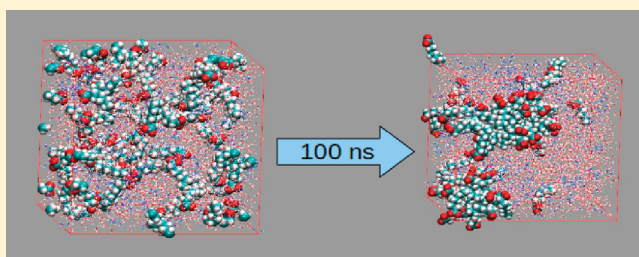
André Farias de Moura,^{*,†} Kalil Bernardino,[†] Osmair Vital de Oliveira,[‡] and Luiz Carlos Gomide Freitas[†]

[†]Departamento de Química, Universidade Federal de São Carlos, CP 676, São Carlos, SP, Brazil, CEP 13565-905

[‡]Instituto Federal de Educação, Ciência e Tecnologia do Espírito Santo, Campus Vila Velha, Av. Ministro Salgado Filho, S/N^o, Vila Velha, ES, Brazil, CEP 29106-010

ABSTRACT: The effects of urea on self-assembling remains a challenging topic on surface chemistry, and computational modeling may have a role on the unraveling of the molecular mechanisms underlying these effects. Bearing that in mind, we performed a set of molecular dynamics simulations to assess the effects of urea on the self-assembling properties of sodium octanoate, an anionic surfactant, as compared to the aggregation of the same surfactant in pure water as the solvent. The concentration of free monomers increased 3-fold in the presence of urea, in agreement with the accepted view that urea should increase monomer solubility.

Regarding the size distribution of micellar aggregates, the urea solution favored smaller micelles and a narrower distribution. Preferential solvation by either water or urea changed along the surfactant molecules, from urea-rich shells around apolar atoms at the end of the hydrophobic tails to nearly no urea at the polar headgroups. This solvation profile is consistent with two different hypotheses from the literature: on one hand, urea molecules interact directly with apolar atoms from the hydrophobic tails, acting as a surfactant, and on the other hand the presence of urea molecules increases the hydration of polar sites. Another important observation regards the solvent structure, which exhibits a complex composition profile around both water and urea molecules. Although the solvent structure was appreciably different in each case, the free energy calculations for the dissociation of a pair of octanoate molecules pointed to a purely enthalpic free energy loss in urea solution, a finding that does not lend support to the third hypothesis that is often claimed as accounting for the urea effects, namely, that urea disrupts water structure and that this structural change decreases the hydrophobic effect due to an entropy change. The presence of urea had no significant effect on the molecular structure of the surfactant molecules, although it caused chain dynamics to become slower. The overall picture arising from the molecular-scale data extracted from our computational models is somewhat different from the traditional views about the structural and dynamical features of self-assembled surfactant systems, pointing out the need for more studies on other self-organized systems using a realistic model system as a way to achieve a more detailed picture.



INTRODUCTION

Self-assembling processes play a central role in research areas as diverse as nanotechnology and biophysics.¹ However, the complex and extended nature of real systems makes it difficult to obtain a detailed picture of the aggregation phenomena involved. Instead, smaller systems have been used as models in both experimental and theoretical investigations of the origins of self-assembling. Aqueous solutions of amphiphilic molecules are among the most frequently used systems for this purpose due to their ability to form several self-assembled structures, ranging from small spheroid aggregates (e.g., micelles) to large assemblies (e.g., monolayers, bilayers, and vesicles).²

Urea has long been known to decrease the stability of self-assembled and self-organized structures in aqueous solution.^{3,4} For instance, it acts as a protein denaturant and increases the critical micelle concentration of amphiphilic molecules regardless of their chemical nature. The origins of urea's ability to modulate self-assembling processes remain a controversial issue, and at least three mechanisms have been proposed during the past four decades. Two of them focus on the so-called hydrophobic

effect, suggesting that urea molecules either interact directly with the hydrophobic regions of amphiphilic molecules, thus increasing their solubility in the aqueous environment,³ or play the role of a structure-breaking solute that weakens the hydrophobic effect by decreasing the extent of the hydrogen bond network of water molecules.⁴ More recently, Dias et al. proposed a new mechanism that regards the increased solvation of the polar and ionic portions of the system as the origins of the observed effects of added urea on self-assembled and self-organized systems.⁵

It should be noted that all three mechanisms may give plausible explanations to several different macroscopic data (for instance, see the general discussion of liquid water models by Frank⁶), although they still lack direct evidence from molecular-scale measurements. Thus, it is difficult to unequivocally assess the validity of each hypothesis. Computer simulations have become increasingly accepted in recent years as the tools of choice to

Received: July 13, 2011

Revised: October 7, 2011

Published: October 25, 2011

tackle problems like this, in which detailed knowledge of the local structure of solvent molecules around solutes is necessary.

Theoretical investigations using molecular dynamics simulations have been performed during the last two decades to assess the effects of urea on the structure and energetics of aqueous urea solutions,^{7–11} proteins and peptides,^{12–17} and small apolar molecules.^{18–21} As regards the effects of urea on the stability of micellar solutions, to the best of our knowledge there has been no attempt to use a realistic model system to assess the microscopic details regarding the atomic-level effects of urea on the self-assembling of surfactant molecules. We aim at filling this gap presenting below the results of a 100 ns-long molecular dynamics simulation of the sodium octanoate micellar system in 4.4 mol L⁻¹ urea solution, comparing the solvation features with those obtained for the same micellar system in aqueous solution. This micellar solution has been extensively studied by means of molecular dynamics simulations,^{22–28} mostly due to the small size of the aggregates and the high surfactant concentrations, both characteristics making this system suitable for computer investigations.

METHODOLOGY

Two model system were assembled, one consisting of 60 octanoate anions, 60 sodium counterions, 330 urea molecules, and 2970 water molecules, and another without urea and 3300 water molecules as the solvent. The solvent composition for the former was chosen to yield a concentration of urea molecules in the range experimentally used to induce the breakdown of self-assembled structures, and both system had a surfactant concentration well above the critical micelle concentration to ensure the self-assembling of the octanoate anions. All molecules were randomly rotated and randomly placed into a cubic box, avoiding strong repulsive contacts on the basis of atom–atom cutoffs, typically 0.2 nm. The molecular geometries and interaction parameters were described using the OPLS-AA forcefield²⁹ for the octanoate anions and the urea molecules, the SPC water model,³⁰ and Åqvist's parameters³¹ for the sodium cations. The atom numbering employed for octanoate in the discussions below is presented in Figure 1. No geometric constraint was imposed to the molecules. The nonbonded interactions were truncated at 1.5 nm, using the particle mesh Ewald method^{32,33} to treat the long-range electrostatic potential beyond cutoff distance and a shift function for the Lennard-Jones interactions. This combination of forcefield and simulation parameters has been described and validated elsewhere.²²

The initial structure was optimized using the steepest descent algorithm to minimize the maximum force in the system. The energy minimization and the simulations were performed using the GROMACS suite (version 4.0.5).^{34–36} The weak coupling scheme of Berendsen³⁷ was used for the temperature ($T = 300$ K and $\tau_T = 0.1$ ps) and the pressure ($p = 1$ bar, $\tau_p = 1.0$ ps, and $\kappa = 4.5 \times 10^{-5}$ bar⁻¹). A 100 ns-long production run was obtained using a 1.0 fs time step for the integration of the equations of motion and updating the neighbors list every tenth step. All the analyses reported below were done using the last 60 ns of the molecular dynamics simulation, saving coordinates at 1 ps intervals.

Four other systems were studied for the purpose of comparison: one octanoate anion in aqueous solution, one octanoate in urea solution, one octane molecule in aqueous solution, and pure octane. These simulation were performed using the same set of parameters employed for the micellar systems described above. Simulation boxes for the molecules in dilute solution contained

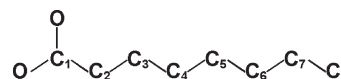


Figure 1. Numbering of the octanoate heavy atoms used in the analyses.

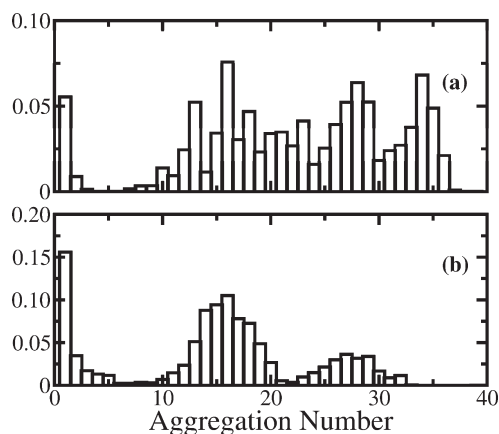


Figure 2. Frequency distribution of the aggregation number of octanoate molecules: (a) aqueous solution; (b) urea solution.

1000 solvent molecules (either pure water or 1:9 urea/water binary mixture) and achieved 100 ns to ensure proper sampling of both structural and dynamical features, whereas the pure octane system comprised 256 molecules and achieved a total integration time of 10 ns.

Besides these equilibrium molecular dynamics simulations, a set of metadynamics simulations were performed to assess the free energy surface for the association of a pair of octanoate anions in solution. A stable octanoate dimer was taken from the previous simulation and was placed in a cubic box with 2500 solvent molecules and 2 sodium counterions, the solvent being either pure water or a water/urea solution with the same molar ratio chosen for the equilibrium simulations. After energy minimization of each system, a 500 ps trajectory was performed, and three low-energy structures were chosen for the free energy calculations. Metadynamics simulations were performed on these systems using the algorithm proposed by Laio and Parrinello³⁸ as implemented in the PLUMED plugin,³⁹ which was coupled to the GROMACS simulation engine. The metadynamics parameters were taken from Laio et al.⁴⁰ ($\Delta t = 0.1$ ps, $\delta s = 0.05$ nm, and $w = 0.35$ kJ mol⁻¹), using the center of mass of each monomer as the collective variables. The free energy of association for the octanoate dimer was computed at five different temperatures (290, 295, 300, 305, and 310 K), to estimate enthalpy and entropy contributions to the association free energy.

RESULTS AND DISCUSSION

To the best of our knowledge, there has been no experimental study on the properties of sodium octanoate micellar solutions in the presence of urea molecules. Nonetheless, this model system has long been investigated by means of molecular dynamics simulations, giving detailed structural information to rationalize the effects of urea molecules in the present work.

We have previously shown that octanoate micelles in aqueous solution present a highly dynamic structure, characterized by the presence of monomers, small aggregates, small micelles, and larger

micelles. Except for the larger aggregates, these structural entities were short-lived, and monomers were exchanged between the solution and the aggregates throughout the simulation.²² In the present work, we have not employed previously assembled octanoate aggregates, increasing considerably the relaxation time needed to equilibrate the model systems. This was especially true for the system containing urea, which reached structural and energetic equilibrium only after ca. 40 ns. After equilibrium was attained, we computed the aggregate size distribution for both systems and found out that the presence of urea molecules induced the formation of a few well-defined populations instead of the broad distribution observed for the micellar system in aqueous solution (Figure 2). We also computed the distributions for the radius of gyration of the aggregates in water and in urea aqueous solution. Visual inspection showed that both systems evolved to form three micellar aggregates surrounded by either a few monomers or small pre-micellar oligomers, thus only the three largest aggregates were considered to compute the distribution of the radius of gyration, which is a reasonable simplification since these aggregates accounted for ca. 90% of the octanoate molecules after both systems attained equilibrium. The major feature emerging from these histograms was the change from a bimodal distribution in pure water to one with a single population of smaller aggregates in the presence of urea (Figure 3). It is noteworthy that the fraction of free monomers became nearly 3-fold larger in aqueous urea solution, a finding consistent with the accepted view that urea increases the stability of free monomers in solution, a plausible explanation for the experimental increase of critical micelle concentration values in the presence of this solute. It also should be noted that fewer monomer exchanges occurred in the presence of urea molecules as compared to the aqueous solution (results not shown here); i.e., the aggregates were structurally and dynamically more stable.

The solvation structure is a key point of the different models that try to explain the effects of added urea on the micellar structure. To check the validity of each model, we shall be concerned with the local solvent structure along the surfactant molecules (the numbering of the octanoate carbon atoms that will be used throughout the discussions was presented in Figure 1) and around the counterions. We shall also consider how solvent molecules are arranged, to get some insight into the way that urea molecules may disturb the water structure within this complex liquid system.

The local structure in any complex fluid may be conveniently characterized by the radial distribution functions of sites B around reference sites A

$$g_{AB}(r) = \frac{\rho_{AB}(r)}{\rho_{AB}} \quad (1)$$

where $\rho_{AB}(r)$ is the local concentration of particles B around reference particles A at distance r and ρ_{AB} is the concentration for the whole system.

The radial distribution functions of the water molecules' oxygen atoms around the octanoate methyl carbon atom presented values below unity (Figure 4), indicating that this hydrophobic site does not interact strongly with water molecules. The small correlation peak around 0.38 nm defines the first solvation shell, and the curve calculated for the micellar system in pure water attains smaller values in the range of distances considered, meaning that the interaction between water molecules and the carbon atom C_8 is more favorable in the presence of urea. Care should be taken regarding the last statement because it does not necessarily mean that there are more water molecules around carbon atom C_8 . Instead, the

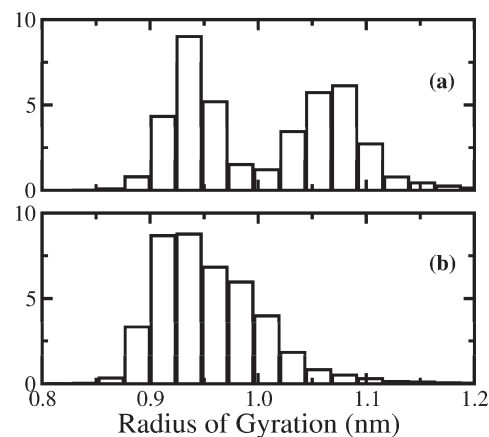


Figure 3. Frequency distribution of the radius of gyration of octanoate aggregates: (a) aqueous solution; (b) urea solution.

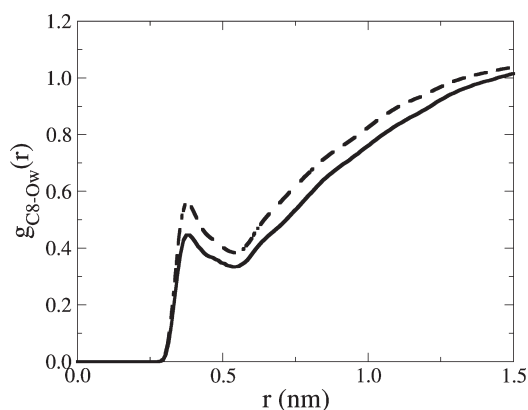


Figure 4. Radial distribution functions of the oxygen atoms of water molecules around methyl carbon atoms C_8 of octanoate molecules in aqueous solution (solid line) and in urea solution (dashed line).

correct interpretation is rooted in eq 1; i.e., given the average concentration for the species considered, the correlation function defines the degree of deviation of the local concentration from this ideal value. The average number of neighbors may be evaluated by the integral

$$CN_{AB} = \int_{r_1}^{r_2} 4\pi r^2 \rho_{AB} g_{AB}(r) dr \quad (2)$$

where CN_{AB} stands for the cumulative number of neighbors between distances r_1 and r_2 , with $r_1 = 0$ nm in both cases. For the system in aqueous solution, $r_2 = 0.55$ nm, yielding 5.7 water molecules in the first hydration shell around carbon atom C_8 , as compared to 5.5 water molecules for the system in urea solution ($r_2 = 0.54$ nm). Thus, the higher correlation value did not mean more water molecules in this case.

Two considerations must be made regarding the number of water molecules around the hydrophobic sites. First, the figures we obtained may seem large for an atom belonging to the octanoate hydrophobic tails, but a sphere with radius 0.54 nm should have nearly 20 water molecules for an ideal homogeneous system. Second, the water molecules around carbon atoms C_8 did not enter into the hydrophobic core, but the tails spent some time at the aqueous interface instead, not to mention the presence of free monomers in solution, which are far more hydrated than the

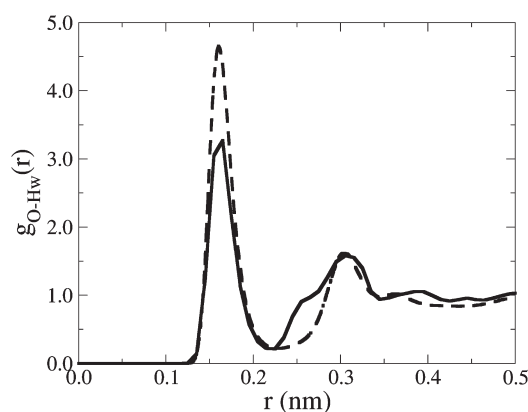


Figure 5. Radial distribution functions of the hydrogen atoms of water molecules around oxygen atoms of octanoate molecules in aqueous solution (solid line) and in urea solution (dashed line).

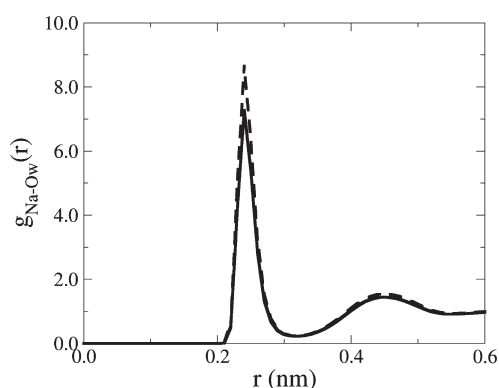


Figure 6. Radial distribution functions of the oxygen atoms of water molecules around sodium atoms in aqueous solution (solid line) and in urea solution (dashed line).

aggregated molecules. Thus, our findings are consistent with the fact that hydrophobic sites are generally buried within micellar aggregates, with little contact with water molecules, no matter whether or not urea molecules are present.

In contrast to the hydrophobic methyl groups, the octanoate headgroups are exposed to the aqueous medium. The headgroups carry a full negative charge located at both oxygen atoms, which act as hydrogen-bond acceptors and interact strongly with the sodium counterions in solution. The radial distribution functions of water hydrogen atoms around the octanoate oxygen atoms present well-defined peaks around 0.18 nm (Figure 5), characterizing the presence of hydrogen bonds. The height of the correlation peak increased in the presence of urea, although the cumulative number of water hydrogen atoms in the first hydration around octanoate oxygen atoms decreased from 3.0 in aqueous solution to 2.7 in urea solution, mostly due to the decrease in the average number density of water molecules in the system containing urea. These figures might lead one to the conclusion that octanoate headgroups are less hydrated in urea solution as compared to the aqueous solution, but the difference between the radial distribution functions suggests that the water molecules in the urea solution interact more favorably with the polar atoms of octanoate molecules. It is worthy mentioning that the second correlation peaks of the radial distribution function of water hydrogen atoms around

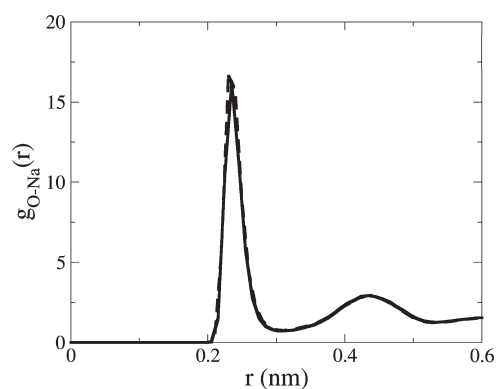


Figure 7. Radial distribution functions of the sodium atoms around oxygen atoms of octanoate molecules in aqueous solution (solid line) and in urea solution (dashed line).

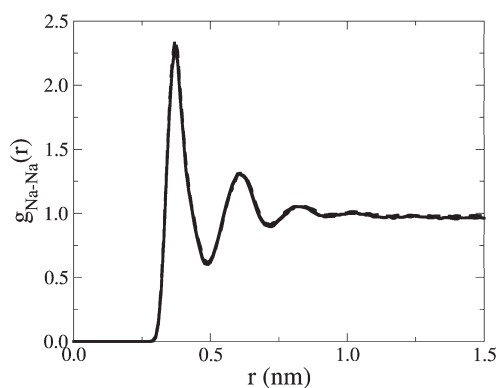


Figure 8. Radial distribution functions of the sodium atoms around other sodium atoms in aqueous solution (solid line) and in urea solution (dashed line).

octanoate oxygen atoms changed considerably in the presence of urea, indicating that the effect of this solute may well reach solvation shells beyond the first one. Similar conclusions may be drawn for the distribution of water oxygen atoms around sodium counterions (Figure 6). Altogether, these findings are consistent with the views of Dias et al.⁵ that ionic and polar groups should be more hydrated in the presence of urea. On the other hand, the correlation functions for the counterions did not present any significant difference in the presence of urea, both for the distribution of sodium cations around the octanoate oxygen atoms (Figure 7) and for the distribution of sodium atoms around each other (Figure 8). At first sight, these findings are not consistent with experimental observations that indicate the increase of the dissociation degree of counterions in concentrated urea solutions, but correlation functions cannot be directly compared with the experimental results regarding the dissociation degree because radial distribution functions describe the correlation between pairs of atoms, not the correlation between atoms and micellar surfaces.

We also verified that the structure of water molecules was affected by the presence of urea molecules, as indicated by the radial distribution functions of water oxygen atoms around other water oxygen atoms (Figure 9). The peak around 0.28 nm is characteristic of hydrogen-bonded water molecules, and there is an increase of the correlation peak height in the presence of urea molecules, once again in agreement with the hypothesis of Dias et al.

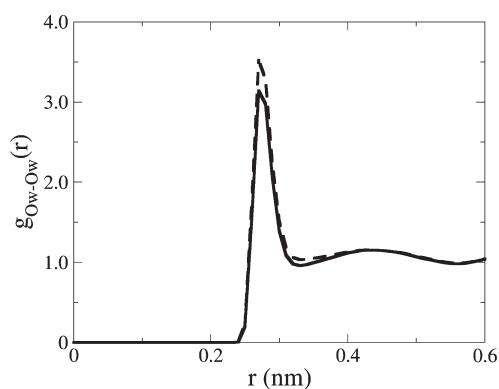


Figure 9. Radial distribution functions of the oxygen atoms of water molecules around the oxygen atoms of other water molecules in aqueous solution (solid line) and in urea solution (dashed line).

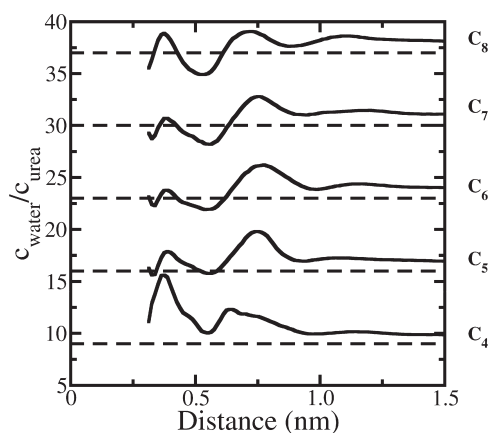


Figure 10. Ratio between the local concentration of water molecules (c_{water}) and the local concentration of urea molecules (c_{urea}) around apolar octanoate carbon atoms. The dashed lines stand for the bulk values (data have been displaced vertically for clarity).

that urea would strengthen the interactions among polar and ionic portions of the system.⁵

To further investigate the structure of the solvent, we calculated the local concentration of urea around some reference atomic sites. We considered the solvent as composed of water and urea molecules and counted one molecule within a spherical shell of radius r and thickness dr whenever the reference atom (the oxygen atom for both water and urea) was found inside this volume element. Varying the distance r , we computed the number of water and urea molecules between r and $r + dr$, $N_{\text{water}}(r)$ and $N_{\text{urea}}(r)$, respectively, allowing the local concentration ratio at position r to be expressed as

$$\frac{c_{\text{water}}}{c_{\text{urea}}} = \frac{N_{\text{water}}}{N_{\text{urea}}} \quad (3)$$

where c_{water} and c_{urea} stand for the local concentration of water and urea, respectively. We dropped the r from the expression above for clarity, but it should be kept in mind that it refers to the local concentration at r . From the model system composition described above, the ideal value would be $c_{\text{water}}/c_{\text{urea}} = 9$ (larger values indicate a preferred local solvation by water molecules, whereas smaller values indicate a preferential urea solvation).

The hydrophobic tails presented a set of interesting solvation profiles (Figure 10). The terminal methyl carbon atom (C_8) and

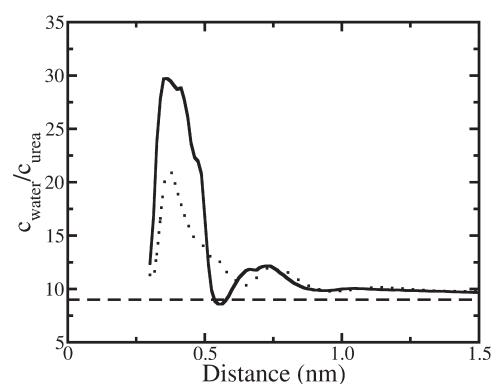


Figure 11. Ratio between the local concentration of water molecules (c_{water}) and the local concentration of urea molecules (c_{urea}) around polar octanoate carbon atoms C_2 (solid line) and C_3 (dotted line). The dashed line stands for the bulk value.

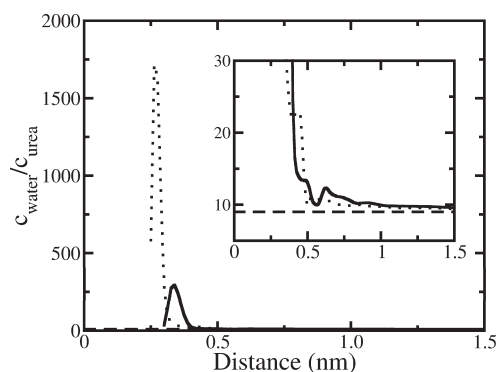


Figure 12. Ratio between the local concentration of water molecules (c_{water}) and the local concentration of urea molecules (c_{urea}) around octanoate carboxylic carbon atom C_1 (solid line) and carboxylic oxygen atoms (dotted line). The dashed line stands for the bulk value.

the next two methylene groups (C_7 and C_6) presented an alternation between urea-rich and water-rich solvation shells, whereas the next two carbon atoms (C_5 and C_4) presented only water-rich solvation shells. These atoms share the same set of forcefield parameters, so the differences in solvent composition cannot be ascribed to the direct interaction between these atomic sites and the solvent molecules. A more plausible explanation for the observed differences is the effect of the local chemical environment; i.e., atoms closer to the polar headgroups (C_4) become more hydrophilic as compared to other similar atoms (C_6 and C_7) that are farther from the headgroups and surrounded almost exclusively by other hydrophobic groups. Thus, amphiphilic molecules present a gradual change between hydrophobic and hydrophilic regions.

The solvation shell becomes increasingly richer in water as we move along the octanoate aliphatic tail closer to the headgroup. The solvent around the methylene carbon atoms C_2 and C_3 never became richer in urea than the average value (Figure 11). This tendency reaches its maximum at the headgroup atoms (Figure 12), around which the concentration of water is much larger than the urea concentration (it should be 9 times larger in an ideal system). A similar trend was observed for the solvent composition around sodium atoms as well (Figure 13).

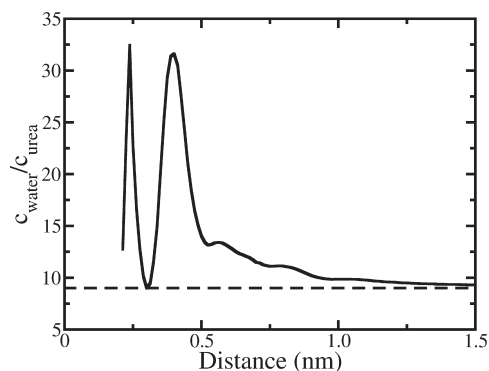


Figure 13. Ratio between the local concentration of water molecules (c_{water}) and the local concentration of urea molecules (c_{urea}) around sodium atoms. The dashed line stands for the bulk value.

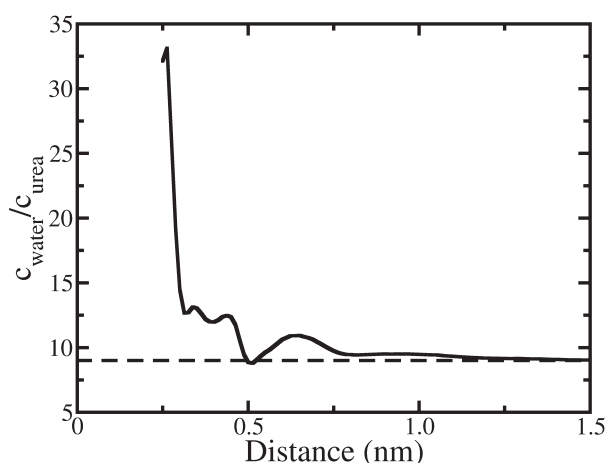


Figure 14. Ratio between the local concentration of water molecules (c_{water}) and the local concentration of urea molecules (c_{urea}) around water oxygen atoms. The dashed line stands for the bulk value.

The change in solvent composition along the octanoate molecules is consistent with the hypothesis that urea interacts directly with the hydrophobic atoms of amphiphilic molecules. At the same time, the pronounced enrichment of water near polar atoms corroborates the views of Dias et al. that urea makes water molecules interact more favorably with the polar moiety.⁵

At last, we must consider how urea affects the solvent itself to check if the simulations give any support to the third hypothesis that urea disrupts the three-dimensional hydrogen bond structure of water, thus weakening the hydrophobic effect. The solvent composition profile around water molecules presented only water-rich shells (Figure 14), whereas the solvent structure around urea molecules presented both a water-rich at short distances due to hydrogen bonding followed by a urea-rich region (Figure 15). In both cases, the short-range water enrichment is significant and points to a disturbed water structure. It should be noted that urea molecules are bulkier than water molecules, so that their presence hinders the approach of other water molecules, thus partly breaking the water hydrogen bond network, as reported elsewhere.⁴¹

The radial distribution functions and the local concentration functions give support to the idea that the solvent structure does not resemble that of pure water as a great amount of urea is added. Nonetheless, this structural information does not allow any clear

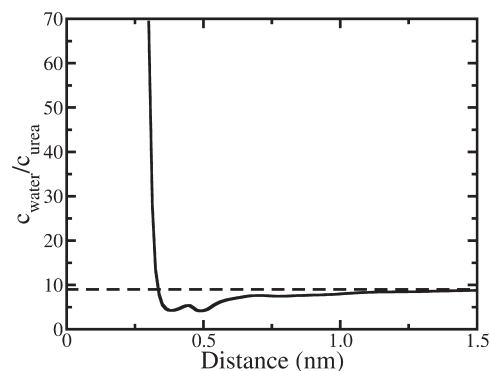


Figure 15. Ratio between the local concentration of water molecules (c_{water}) and the local concentration of urea molecules (c_{urea}) around urea oxygen atoms. The dashed line stands for the bulk value.

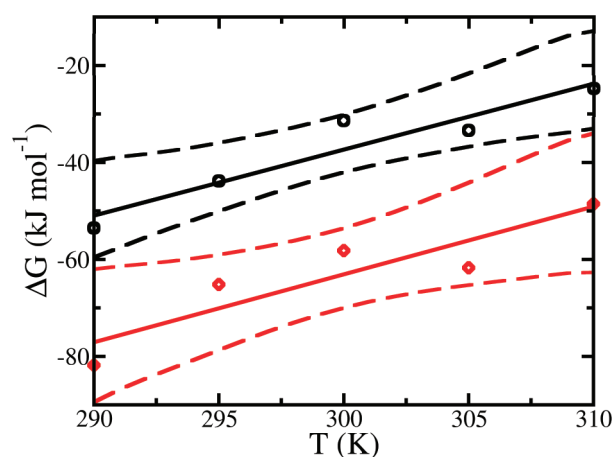


Figure 16. Free energy of association for a dimer of octanoate molecules in aqueous solution (red \diamond) and in urea solution (black \circ). The solid lines stand for the linear regression estimates, whereas the dashed lines stand for the confidence bands of linear regression estimates at the level of 0.95 of probability.

thermodynamical reasoning regarding the effects of urea on the free energy landscape of the surfactant association process. As a matter of fact, equilibrium molecular dynamics simulations are not adequate for this kind of investigation, as the system spends most of the time at the low-lying energy states. Several different approaches have been proposed to overcome this intrinsic limitation, allowing a more thorough sampling of thermodynamically less probable states. One such approach that is adequate for the present investigation is the metadynamics algorithm proposed by Laio and Parrinello³⁸ that adds repulsive Gaussian potentials along a chosen set of arbitrary coordinates, the so-called collective variables, forcing the system out of its global and local minima. The center of mass distance separating two surfactant molecules is an adequate coordinate describing the self-assembling of two monomers into a dimer. As the dimer is the more stable form in solution with respect to the monomeric state, the metadynamics began from an equilibrated dimer in solution, forcing the system into its monomeric state by means of the added Gaussian potentials. At each temperature, three simulations were performed starting from different initial configurations of the model system. Each simulation at the same temperature yielded a different value for the free

energy of association of octanoate anions, the most negative value being considered as the closest estimate to the global minimum of the free energy surface at that temperature.

The free energy values for the octanoate association are more negative in aqueous solution than in urea solution (Figure 16), a finding that is consistent with the conclusions drawn from the size distribution histograms (Figure 2) that indicated an increased stability of the monomers in urea solution. The linear regression analysis performed on each data set pointed to a nearly equal negative entropy contribution for the association process in aqueous solution ($-(1.4 \pm 0.4) \text{ kJ mol}^{-1} \text{ K}^{-1}$) and in urea solution ($-(1.36 \pm 0.26) \text{ kJ mol}^{-1} \text{ K}^{-1}$), meaning that the association of octanoate is not entropy driven in both systems and that the presence of urea has no significant effect on the magnitude of the entropy of association whatsoever. Thus, our computational experiments do not lend support to the hypothesis claiming that the known effects of urea on the self-assembling is entropic in nature and should be ascribed to the breakdown of the three-dimensional structure of water, although the structure was actually disrupted by urea molecules. On the other hand, the difference between the linear regression estimates for the enthalpy contributions amounts to ca. 25 kJ mol^{-1} of free energy loss at 300 K in the presence of urea.

Zangi et al.⁴² reported similar findings for purely hydrophobic model systems studied by molecular dynamics simulations. Their general conclusions match ours, as they report the direct interaction between urea and the hydrophobic sites to be the dominant structural feature related to the decreased thermodynamical stability of hydrophobic aggregation in urea solution as compared to aqueous solutions. They computed the free energy of dissociation for a pair of model hydrophobic plates in water (ΔG_{water}) and in 7 M urea solution (ΔG_{urea}) to estimate the urea effect on the stability of the dimer as $\Delta\Delta G = \Delta G_{\text{urea}} - \Delta G_{\text{water}}$ (negative values of $\Delta\Delta G$ indicating that urea destabilized the aggregated state). These free energy calculations yielded both positive and negative $\Delta\Delta G$ values, depending on the intensity of the dispersion interactions of the hydrophobic sites comprising the plates (small magnitude dispersion attraction leading to positive $\Delta\Delta G$ values). Although $\Delta\Delta G$ changed sign as the dispersion interaction became stronger, all the considered model systems presented a negative $\Delta\Delta H$ term ranging from ca. -10 to ca. -100 kJ mol^{-1} , comparable to the magnitude of our estimate for the enthalpy contribution for the free energy difference in the presence of urea (our result was positive as we chose to describe the association process instead). On the other hand, Zangi et al. found a negative $T\Delta\Delta S$, meaning that the entropic contribution tends to increase the hydrophobic effect in urea solution as compared to pure water, becoming the dominant effect for small $\Delta\Delta H$ values. This finding and the results obtained for the octanoate dimer are at odds, as our estimates for ΔS_{urea} and ΔS_{water} were statistically indistinguishable, pointing to $T\Delta\Delta S \approx 0 \text{ kJ mol}^{-1}$. Thus, urea affects only the enthalpy of association/dissociation for a sodium octanoate dimer in solution.

Besides affecting the free energy landscape, it is a worthy question whether urea affects the internal structure of the micellar aggregates. A typical phenomenological model considers the surfactants' hydrophobic tails to be packed into a liquid hydrocarbon-like droplet, with the polar headgroups anchored at the hydrophilic–hydrophobic interface and pointing to the aqueous medium.² The dihedral angles formed by four consecutive atoms along the octanoate chains may give some insight into the differences between the aggregated molecules and the monomers

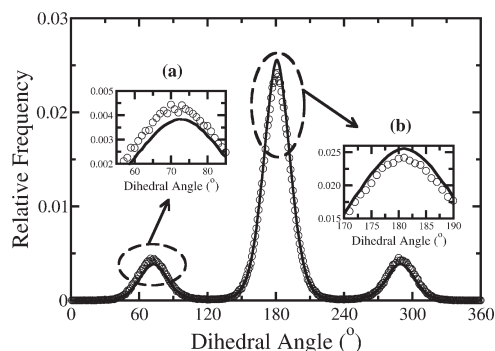


Figure 17. Dihedral angle distribution for the carbon atoms $C_5-C_6-C_7-C_8$ of octanoate molecules in aqueous solution. The solid lines stand for the micellar solution and the open circles stand for one monomer in solution. Insets (a) and (b) are enlarged views for peaks corresponding to the gauche and trans conformations, respectively.

in solution. For instance, the dihedral angle defined by the atoms $C_5-C_6-C_7-C_8$ for a single monomer in aqueous solution had a slightly lower frequency count of trans conformations than the average value observed for the micellar system in aqueous solution (Figure 17). This finding is qualitatively consistent with the view that the hydrophobic effect should favor apolar tails with more compact conformations, thus increasing the relative population of gauche conformations at the expense of a decrease in the population of trans conformations. Nearly identical distributions were obtained for this dihedral in urea solution for both the monomer and the micellar system (results not shown), indicating that aggregation had a slight effect on the tail conformation, whereas the presence of urea had no noticeable effect whatsoever. The overall conformational change was estimated by the average radius of gyration for the octanoate anions in each model system and amounted to only 0.005 nm , well below the calculated statistical uncertainty of the average radius of gyration for the monomers in solution. Thus, no significant structural change was captured by the simulations.

Although the structural differences were hardly noticeable in our simulations, the dynamics of the transition between the gauche and trans conformations may change significantly upon micellization. The dynamics of a tail segment may be assessed by the correlation time for the dihedral angle relaxation, obtained from the fitting of the time correlation function for the cosine of the dihedral angles to a single exponential model. For purposes of comparison, we performed a molecular dynamics simulation of one octane molecule in aqueous solution, as well as a simulation of pure octane in the liquid phase. For pure octane, the estimated correlation time was 41.4 ps (as the octane molecule is symmetric, we compared the estimated correlation times for both $C_1-C_2-C_3-C_4$ and $C_5-C_6-C_7-C_8$ dihedrals, allowing the precision to be estimated as less than 0.1 ps), whereas the simulation of one octane molecule in aqueous solution yielded an estimated correlation time of 39.9 ps . As regards octanoate anions in solution, the correlation times for the $C_5-C_6-C_7-C_8$ dihedral changed from 40.3 ps for the monomeric state to 44.1 ps in the micellar system. Thus, the octanoate tails became less flexible upon micellization and were less flexible than the equivalent liquid hydrocarbon. In the presence of urea molecules, the estimated correlation times for the $C_5-C_6-C_7-C_8$ dihedral were 42.5 ps for the monomer and 45.0 ps for the micellar solution, giving support to the idea that surfactant conformational changes were slower in urea solution than in aqueous solution. Correlation times changed along the surfactant molecule (Figure 18), but the

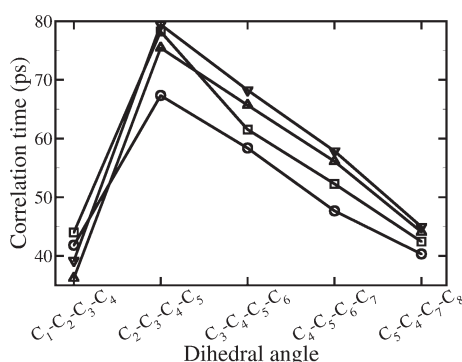


Figure 18. Correlation times for the dihedrals along the octanoate molecules: (○) monomer in aqueous solution; (□) monomer in urea solution; (Δ) micelle in aqueous solution; (▽) micelle in urea solution.

data from the simulations suggest that the mobility decreased in the presence of urea. It also is interesting to note that the atoms closer to the headgroup (C₁–C₂–C₃–C₄ dihedral) presented the lower correlation times in all the model systems that were considered in our study and that this was the only dihedral for which the correlation times decreased upon micellization.

CONCLUSIONS

We performed a set of molecular dynamics simulations to access the effects of added urea on the molecular level structure of anionic micelles in aqueous solution and to obtain a thermodynamical description of the aggregation process. The size distribution of molecular aggregates is consistent with the one point in common among the existing phenomenological models, all of which assume that urea increases the solubility of surfactant molecules in the aqueous solution based on a variety of experimental data. Besides the increased probability of finding monomers in solution, the size distribution also indicated that larger aggregates become less probable in the presence of urea. The urea solution also presented a different hydration pattern of the surfactant molecules as compared to the aqueous solution, with increased probability of finding water molecules near the octanoate molecules.

Urea molecules should not be regarded as an extra solute, being more correct to describe it as a second solvent. From this standpoint, it is reasonable to ask whether or not solvent composition is uniform along the system. We accomplished this investigation computing the local concentration of urea around each atom comprising the surfactant molecules, their counterions, and the solvent molecules, thus making a clear and detailed picture of regions either water-rich or urea-rich. The overall conclusion was that water–urea binary solvent is a highly nonideal solvent mixture, in which a urea-rich solvation shell formed around apolar atoms belonging to the end of the surfactant hydrophobic tails. Both the tail atoms near the headgroups and the headgroups themselves are solvated by water-rich shells. The water enrichment increases as we move along the surfactant molecules toward the oxygen atoms, where the ratio $N_{\text{water}}:N_{\text{urea}}$ reaches the impressive value of 1695:1, as compared to the ideal solution value of 9:1. These figures give a clear indication that urea molecules are rarely near the negative oxygen atoms, an observation that may be ascribed to the bulkier character of urea molecules as compared to water molecules and the fact that they do not have any specific and strong interaction with the headgroup atoms as water molecules do. The same trends hold true for the solvation of the counterions and of water

molecules, but for urea the solvation pattern changes from water-rich at very short distances to a urea-rich environment farther apart.

These facts give support to two out of three hypotheses on the way urea should influence micellar systems, the first claiming that urea would interact directly with the hydrophobic tails and the second claiming that water molecules interact more strongly with polar moieties in the presence of urea. Regarding the third hypothesis suggesting the role of urea as a solvent structure breaker, the free energy surface obtained from a set of metadynamics simulations for the aggregation of an octanoate dimer in solution does not lend support to the view that the hydrophobic effect should be entropic in nature and that urea would change this entropic contribution. The estimated free energy changes suggest a completely different thermodynamical view of the self-assembly of anionic surfactants in aqueous solution and the effect of added urea, pointing to an enthalpy-driven association and to a purely enthalpic change of the association free energy in the presence of urea, leading to a less stable aggregate in urea solution.

The internal structure of the aggregates is not sensitive to the presence of urea molecules in solution, as indicated by the dihedral distributions. Nonetheless, the chain dynamics is sensitive to both the aggregation state of the surfactant molecules and the presence of urea in the solution. The terminal methyl groups seem to be hindered inside the micellar core, moving slower than they would in a liquid hydrocarbon.

AUTHOR INFORMATION

Corresponding Author

*Phone: + 55-16-3351-8090. Fax: + 55-16-3351-8350. E-mail: moura@ufscar.br.

ACKNOWLEDGMENT

We thank FAPESP, CAPES, and CNPq (Brazilian funding agencies) for their financial support.

REFERENCES

- (1) Whitesides, G. M.; Grzybowski, B. *Science* **2002**, *295*, 2418–2421.
- (2) Israelachvili, J. N. *Intermolecular and surface forces*, 2nd ed.; Academic Press: London, 1995.
- (3) Robinson, D. R.; Jencks, W. P. *J. Am. Chem. Soc.* **1965**, *87*, 2462–2470.
- (4) Frank, H. S.; Franks, F. *J. Chem. Phys.* **1968**, *48*, 4746–4757.
- (5) Dias, L. G.; Florenzano, F. H.; Reed, W. F.; Baptista, M. S.; Souza, S. M. B.; Alvarez, E. B.; Chaimovich, H.; Cuccovia, I. M.; Amaral, C. L. C.; Brasil, C. R.; Romsted, L. S.; Politi, M. *J. Langmuir* **2002**, *18*, 319–324.
- (6) Frank, H. S. *Structural Models; Water: a Comprehensive Treatise*, V. I.; Franks, F., Ed.; Plenum Press: New York, 1972.
- (7) Smith, L. J.; Berendsen, H. J. C.; van Gunsteren, W. F. *J. Phys. Chem. B* **2004**, *108*, 1065–1071.
- (8) Mountain, R. D.; Thirumalai, D. *J. Phys. Chem. B* **2004**, *108*, 6826–6831.
- (9) Caballero-Herrera, A.; Nilsson, L. *J. Mol. Struct.: THEOCHEM* **2006**, *758*, 139–148.
- (10) Kokubo, H.; Pettitt, B. M. *J. Phys. Chem. B* **2007**, *111*, 5233–5242.
- (11) Stumpe, M. C.; Grubmüller, H. *J. Phys. Chem. B* **2007**, *111*, 6220–6228.
- (12) Caballero-Herrera, A.; Nordstrand, K.; Berndt, K. D.; Nilsson, L. *Biophys. J.* **2005**, *89*, 842–857.
- (13) Stumpe, M. C.; Grubmüller, H. *J. Am. Chem. Soc.* **2007**, *129*, 16126–16131.

- (14) Rocco, A. G.; Mollica, L.; Ricchiuto, P.; Baptista, A. M.; Gianazza, E.; Eberini, I. *Biophys. J.* **2008**, *94*, 2241–2251.
- (15) Camilloni, C.; Rocco, A. G.; Eberini, I.; Gianazza, E.; Broglia, R. A.; Tiana, G. *Biophys. J.* **2008**, *94*, 4654–4661.
- (16) Smolin, N.; Winter, R. *J. Phys. Chem. B* **2008**, *112*, 997–1006.
- (17) Das, A.; Mukhopadhyay, C. *J. Phys. Chem. B* **2008**, *112*, 7903–7908.
- (18) Lee, M.-E.; van der Vegt, N. F. A. *J. Am. Chem. Soc.* **2006**, *128*, 4948–4949.
- (19) van der Vegt, N. F. A.; Lee, M.-E.; Trzesniak, D.; van Gunsteren, W. F. *J. Phys. Chem. B* **2006**, *110*, 12852–12855.
- (20) Paul, S.; Patey, G. N. *J. Phys. Chem. B* **2007**, *111*, 7932–7933.
- (21) Paul, S.; Patey, G. N. *J. Phys. Chem. B* **2008**, *112*, 11106–11111.
- (22) de Moura, A. F.; Freitas, L. C. G. *Chem. Phys. Lett.* **2005**, *411*, 474–478.
- (23) Jonsson, B.; Edholm, O.; Teleman, O. *J. Chem. Phys.* **1986**, *85*, 2259–2271.
- (24) Watanabe, K.; Ferrario, M.; Klein, M. L. *J. Phys. Chem.* **1988**, *92*, 819–821.
- (25) Watanabe, K.; Klein, M. L. *J. Phys. Chem.* **1989**, *93*, 6897–6901.
- (26) Shelley, J.; Sprik, M.; Klein, M. L. *Langmuir* **1993**, *9*, 916–926.
- (27) Laaksonen, L.; Rosenholm, J. B. *Chem. Phys. Lett.* **1993**, *216*, 429–434.
- (28) de Moura, A. F.; Freitas, L. C. G. *Braz. J. Phys.* **2004**, *34*, 64–72.
- (29) Jorgensen, W. L.; Maxwell, D. S.; Tirado-Rives, J. *J. Am. Chem. Soc.* **1996**, *118*, 11225–11236.
- (30) Berendsen, H. J. C.; Postma, J. P. M.; van Gunsteren, W. F.; Hermans, J. In *Intermolecular Forces*; Pullman, B., Ed.; Reidel: Dordrecht, 1981; p 331.
- (31) Åqvist, J. *J. Phys. Chem.* **1990**, *94*, 8021–8024.
- (32) Darden, T.; York, D.; Pedersen, L. *J. Chem. Phys.* **1993**, *98*, 10089–10092.
- (33) Essmann, U.; Perera, L.; Berkowitz, M. L.; Darden, T.; Lee, H.; Pedersen, L. G. *J. Chem. Phys.* **1995**, *103*, 8577–8592.
- (34) Berendsen, H. J. C.; van der Spoel, D.; van Drunen, R. *Comput. Phys. Commun.* **1995**, *91*, 43–56.
- (35) Lindahl, E.; Hess, B.; van der Spoel, D. *J. Mol. Mod.* **2001**, *7*, 306–317.
- (36) van der Spoel, D.; Lindahl, E.; Hess, B.; Groenhof, G.; Mark, A. E.; Berendsen, H. J. C. *J. Comput. Chem.* **2005**, *26*, 1701–1719.
- (37) Berendsen, H. J. C.; Postma, J. P. M.; DiNola, A.; Haak, J. R. *J. Chem. Phys.* **1984**, *81*, 3684–3690.
- (38) Laio, A.; Parrinello, M. *Proc. Natl. Acad. Sci. USA* **2002**, *99*, 12562–12566.
- (39) Bonomi, M.; Branduardi, D.; Bussi, G.; Camilloni, C.; Provasi, D.; Raiteri, P.; Donadio, D.; Marinelli, F.; Pietrucci, F.; Broglia, R. A. *Comput. Phys. Commun.* **2009**, *180*, 1961–1972.
- (40) Laio, A.; Rodriguez-Forte, A.; Gervasio, F. L.; Ceccarelli, M.; Parrinello, M. *J. Phys. Chem. B* **2005**, *109*, 6714–6721.
- (41) Bertran, C. A.; Cirino, J. J. V.; Freitas, L. C. G. *J. Braz. Chem. Soc.* **2002**, *13*, 238–244.
- (42) Zangi, R.; Zhou, R.; Berne, B. J. *J. Am. Chem. Soc.* **2009**, *131*, 1535–1541.